Chapter 3

Peristaltic Transport of Herschel-Bulkley Fluids in Circular Cylindrical Tubes Caused by Dilating Peristaltic Waves: Application to achalasia

3.1 Introduction

Physiological fluids in living beings are pumped rhythmically by continuous and alternate contractions and relaxations of the walls of the ducts in which fluid pass. This physiological phenomenon is termed as peristaltic pumping. Peristaltic waves causing transportation of the fluid through the muscular tubes is indeed an essential biological mechanism responsible for physiological functions of the various organs of the human body. Peristalsis plays the primary role in the flows of food bolus through oesophagus, chyme through intestines, spermatic fluid through vas deference, embryo through uterine cavity, ovum through female fallopian tube, urine through ureter and blood through small blood vessels. It is an inherent property of many tubular organs of the human body. In some biomedical instruments, such as heart-lung machines, peristaltic motion is used to pump blood and other biological fluids.

Herschel-Bulkley fluids are non-Newtonian fluids that possess a yield stress due to which during deformation the fluid has a plug flow region at times when the local shear is below the yield stress. Once the yield stress is exceeded, the fluid flows with a non-linear stress-strain relationship as a shear-thickening or a shear thinning fluid (Fig. 3.1). Raisin paste, minced fish paste etc. are some examples of edible fluids of this type. Some more edible semi-fluids such as cornstarch in water (dilatant), peanut butter, ketchup (pseudo

plastic) and tomato puri, melted chocolate (Bingham fluid) are special cases of Hurschel-Bulkley fluid (Bourne, 2002). The flow behaviours of these fluids can be examined by this model by considering special cases. Some more fluids possessing this property are paints, plastics, slurries, pharmaceutical products, polymeric solutions, paper pulp and semi-solid materials (Alexandrou et al., 2001). The proposed model can also be valid for industrial and clinical purposes.

The human oesophagus is a flexible muscular tube extending from pharynx to stomach. Its length is about 25-30 cm (Lamb and Griffin, 2005) and the diameter lies between 1.8 cm and 2.1 cm (Joohee et al., 2012). The oesophagus is an upper part of the digestive system. Food is ingested through the mouth and when swallowed passes first into the pharynx and then into the oesophagus. The process of swallowing is a mechanical phenomenon. It begins with chewing and mixing of food in the oral cavity. The complex structural motions within the pharynx forces the food bolus rapidly into the oesophagus and then the process ends with the transport of the bolus to the stomach by the peristaltic contractions of the oesophageal wall.

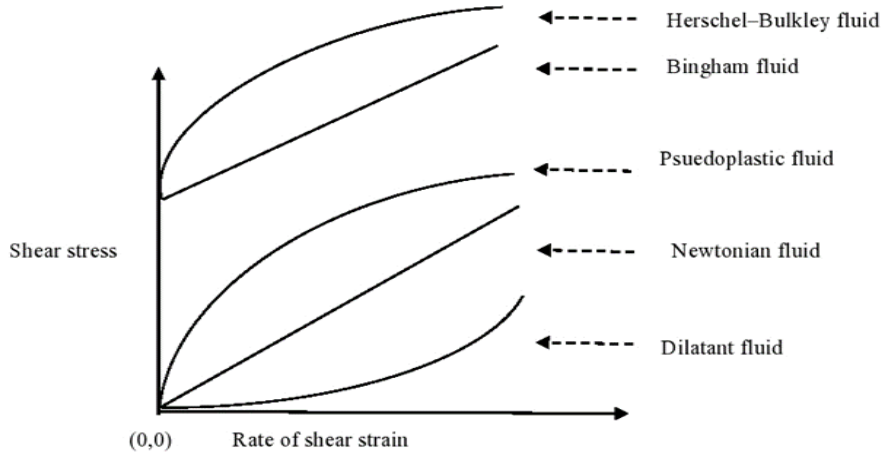

Fig. 3.1 *Pictorial demonstration of Herschel-Bulkley fluid*

Several investigations on the peristaltic transport through circular cylindrical tubes have been carried out by various researchers for Newtonian and non-Newtonian fluid. Li and Brasseur (1993) raised an issue of prime concern that the oesophageal wall undergoes contraction followed by relaxation; but in most of the studies the wall is considered to oscillate about the mean position, i.e., the stationary boundary. They incorporated this correction so that the model can be applied to oesophageal swallowing. It was further

improved by a more suitable model by Misra and Pandey (2001). In all of the models for oesophageal swallowing, the wave amplitude was assumed to be constant by the investigators including Li and Brasseure (1993), Misra and Pandey (2001) and Pandey and Tripathi (2010c, 2011b). Xia et al. (2009) measured oesophageal wall thickness in contracted as well as dilated state through 110 consecutive CT images of adult patients without oesophageal diseases. Kahrilas et al. (1995) located a high pressure zone in the lower part of the oesophagus. The overall conclusion that Pandey et al. (2017) drew by analyzing the data made available by them was that, in the dilated state, the upper oesophagus is thicker while, in the contracted state, the lower oesophagus is thicker. Pandey et al. (2017) also concluded that the change in the thickness in the lower oesophageal wall is more than that in the upper part. Since the peristaltic waves are created by the contraction of circular muscles of oesophagus, a larger thickness of wall is an indication of larger degree of contraction. Hence they modeled the wall equation with increasing wave amplitude. Pandey and Tiwari (2017) studied swallowing of Casson fluid in oesophagus under the influence of peristaltic waves of varying amplitude. The conclusions were in conformity with experimental findings. Motivated by those studies, we attempt to investigate peristaltic transport of Herschel-Bulkley fluid in an oesophagus when the wave amplitude dilates while propagating along the wall. This is because several edible materials physically resemble Herschel-Bulkley properties (Fig.3.1). Vajravelu et al. (2005) analyzed peristaltic flow of Herschel–Bulkley fluid in an inclined tube. Akbar and Butt (2015) also investigated peristaltic motion in a non-uniform channel filled with Herschel-Bulkley fluid. But their investigations are not meant for oesophageal swallowing particularly under the circumstances we intend to investigate.

3.2 Mathematical Formulation

We consider oesophagus as a circular cylindrical tube undergoing peristaltic contraction and relaxation proposed by Pandey et al. (2017) gets modified for the single wave propagation may be given by

$$H'(x',t',k') = \begin{cases} a - \emptyset' e^{k'x'} cos^2 \frac{\pi}{\lambda}(x' - ct'), & \text{during } [t',\ t' + \frac{\lambda}{c}] \\ a - \emptyset' e^{k'x'}, & \text{otherwise} \end{cases} \tag{3.1}$$

where $H', x', t', a, \emptyset', \lambda, k'$ and c respectively denote radial displacement of the wall from the centre line, axial coordinate, time parameter, radius of the tube, amplitude of the

wave supposed to propagate along the wall to create a motion as desired, wavelength, dilation parameter and wave velocity. The geometry is given in Fig. 3.2.

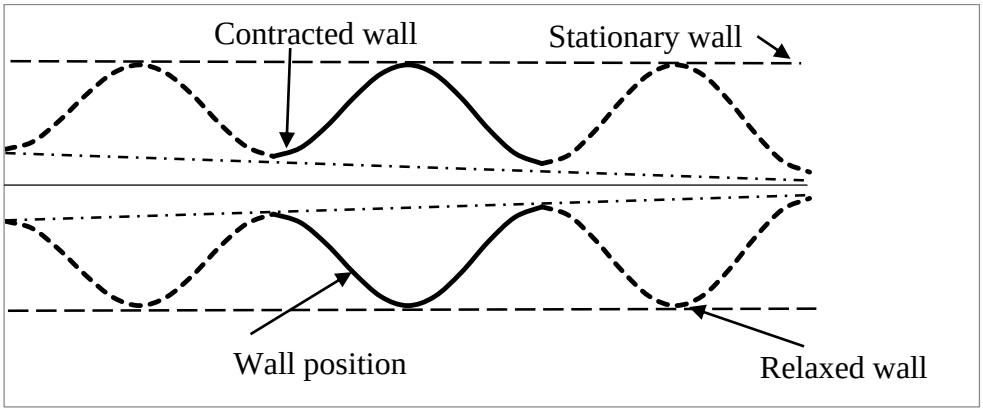

Fig. 3.2 *Geometry of the flow under peristaltic waves of progressively dilating amplitude. The continuous solid wave indicates position of single bolus; similar boluses lagging behind or leading simply symbolize that the previous position and the future position of the bolus.*

The governing equations for the axi-symmetric flow of an incompressible fluid with no body force are given by

$$\rho\left(\frac{\partial}{\partial t'}+u'\frac{\partial}{\partial x'}+v'\frac{\partial}{\partial r'}\right)u' = -\frac{\partial p'}{\partial x'}+\frac{1}{r'}\frac{\partial(r'\tau'_{r'x'})}{\partial r'}+\frac{\partial \tau'_{x'x'}}{\partial x'}, \tag{3.2}$$

$$\rho\left(\frac{\partial}{\partial t'}+u'\frac{\partial}{\partial x'}+v'\frac{\partial}{\partial r'}\right)v' = -\frac{\partial p'}{\partial r'}+\frac{1}{r'}\frac{\partial(r'\tau'_{r'r'})}{\partial r'}+\frac{\partial \tau'_{x'r'}}{\partial x'}-\frac{\tau'_{\theta'\theta'}}{r'}. \tag{3.3}$$

The equation of continuity is

$$\frac{\partial u'}{\partial x'}+\frac{1}{r'}\frac{\partial(r'v')}{\partial r'}=0, \tag{3.4}$$

where $\tau'_{ij}\ (i,j=r',x',\theta'), \rho, u', p', v'$ and r' are the shear stress tensor components, fluid density, axial velocity, pressure, radial velocity, and radial coordinate respectively.

The Herschel -Bulkley fluid model, geometrically presented in Fig. 3.1, is defined as

$$\left.\begin{aligned} \tau'_{r'x'} &= \mu'\left|\frac{\partial u'}{\partial r'}\right|^{n-1}\frac{\partial u'}{\partial r'}+\tau'_0, && \tau'_{r'x'} > \tau'_0 \\ \frac{\partial u'}{\partial r'} &= 0, && \tau'_{r'x'} \le \tau'_0 \end{aligned}\right\}. \tag{3.5}$$

where μ', n and τ'_0 are the flow consistency index (not to be confused with viscosity because the effective viscosity is $\mu' \left|\frac{\partial u'}{\partial r'}\right|^{n-1}$), flow behaviour index and yield stress respectively. We plan to apply long wavelength approximation, stress components other than defined in Eq. (3.5) will get eliminated, for that reason, the rest are not defined here.

The various parameters are non-dimensionalised for dimensional similarity as follows:

$$\left.\begin{aligned} x = \frac{x'}{\lambda}, \quad r = \frac{r'}{a}, \quad t = \frac{ct'}{\lambda}, \quad u = \frac{u'}{c}, \quad v = \frac{v'}{c\alpha}, \quad \alpha = \frac{a}{\lambda}, \\ H = \frac{H'}{a}, \; k = k'\lambda, \tau_0 = \frac{\tau'_0}{\mu'}\left(\frac{a}{c}\right)^n, \tau_{ij} = \frac{\tau'_{i'j'}}{\mu'}\left(\frac{a}{c}\right)^n \quad (i,j = r,x,\theta), \\ l = \frac{l'}{\lambda}, \quad \phi = \frac{\emptyset'}{a}, \quad p = \frac{p'\,a^2}{\mu' c\lambda}, \quad Q = \frac{Q'}{\pi a^2 c}, \quad R_e = \frac{\rho a^n \alpha}{\mu' c^{n-2}}. \end{aligned}\right\} \tag{3.6}$$

where α is a parameter that gives the ratio of the radius of the tube and wavelength, while l, Q and R_e are respectively length of the tube, volume flow rate and Reynolds number.

Introducing the above mentioned dimensionless parameters in Eqs. (3.1)-(3.5) followed by the application of the long wavelength approximation, Eqs. (3.1)-(3.5) under low Reynolds number approximation reduce respectively to the following dimensionless form

$$H(x,t,k) = \begin{cases} 1 - \emptyset e^{kx} cos^2 \pi(x-t), & \text{during } [t,\ t+1\,] \\ 1 - \emptyset e^{kx}, & \text{otherwise} \end{cases}. \tag{3.7}$$

$$\frac{\partial p}{\partial x} = \frac{1}{r}\frac{\partial (r\tau_{rx})}{\partial r} \tag{3.8}$$

$$\frac{\partial p}{\partial r} = 0 \tag{3.9}$$

$$\frac{\partial u}{\partial x} + \frac{1}{r}\frac{\partial (rv)}{\partial r} = 0 \tag{3.10}$$

$$\left.\begin{aligned} \tau_{rx} = \left|\frac{\partial u}{\partial r}\right|^{n-1}\frac{\partial u}{\partial r} + \tau_0, \qquad \tau_{rx} > \tau_0 \\ \frac{\partial u}{\partial r} = 0, \qquad\qquad\qquad \tau_{rx} \le \tau_0 \end{aligned}\right\} \tag{3.11}$$

The following boundary conditions, given in dimensionless form (dimensional counterparts being similar) are imposed on the governing equations:

no slip condition on inner surface of the oesophagus, i.e $u(r,x,t)|_{r=H} = 0$, (3.12)

radial velocity at the wall of the oesophagus, i.e $v(r,x,t)|_{r=H} = \frac{\partial H}{\partial t}$, (3.13)

absence of any radial velocity in the plug flow region, i.e $v(r,x,t)|_{r=H_{pl}} = 0$, (3.14)

regularity condition, i.e $\left.\frac{\partial u}{\partial r}\right|_{r=H_{pl}} = 0$, (3.15)

where H_{pl} is the radius of the plug flow region defined by

$$H_{pl} = \frac{2\tau_0}{\frac{\partial p}{\partial x}}. \tag{3.16}$$

3.3 Solution

Integrating Eq. (3.8), with Eq. (3.9) taken into consideration, with respect to r, we get

$$\tau_{rx} = \frac{r}{2}\frac{\partial p}{\partial x} + \frac{A(x,t)}{2}, \tag{3.17}$$

where $A(x,t)$ is an arbitrary function of x and t.

Now, using Eq. (3.11) in Eq. (3.17) and then applying condition (3.15), we obtain

$$\frac{\partial u}{\partial r} = \left(\frac{r}{2}\frac{\partial p}{\partial x} - \tau_0\right)^{\frac{1}{n}}.$$

Integrating it with respect to r and applying the no-slip condition given by Eq. (3.12), the axial velocity may be, in view of Eq. (3.7), given by

$$u(x,r,t) = \frac{\frac{\partial p}{\partial x}\left|\frac{\partial p}{\partial x}\right|^{\frac{1}{n}-1}}{2^{\frac{1}{n}}\left(\frac{1}{n}+1\right)}\left[\left\{r - H_{pl}\right\}^{\frac{1}{n}+1} - \left\{H - H_{pl}\right\}^{\frac{1}{n}+1}\right]. \tag{3.18}$$

The plug flow velocity is obtained by putting $r = H_{pl}$ in Eq. (3.18) and is given by

$$u_{pl}(x,t) = -\frac{\frac{\partial p}{\partial x}\left|\frac{\partial p}{\partial x}\right|^{\frac{1}{n}-1}}{2^{\frac{1}{n}}\left(\frac{1}{n}+1\right)}\left\{H - H_{pl}\right\}^{\frac{1}{n}+1}. \tag{3.19}$$

Solving the continuity Eq. (3.10) together with Eq. (3.14) and then dividing resulting equation by r, we obtain the radial velocity

$$v(x,r,t) = \frac{\left|\frac{\partial p}{\partial x}\right|^{\frac{1}{n}-1}\frac{\partial H}{\partial x}\frac{\partial p}{\partial x}\{H-H_{pl}\}^{\frac{1}{n}}r}{2^{\left(\frac{1}{n}+1\right)}} + \frac{\frac{1}{n}\left|\frac{\partial p}{\partial x}\right|^{\frac{1}{n}-2}\frac{\partial p}{\partial x}\frac{\partial^2 p}{\partial x^2}\{H-H_{pl}\}^{\frac{1}{n}+1}r}{\left(\frac{1}{n}+1\right)2^{\left(\frac{1}{n}+1\right)}} - \frac{\frac{1}{n}\left|\frac{\partial p}{\partial x}\right|^{\frac{1}{n}-2}\frac{\partial p}{\partial x}\frac{\partial^2 p}{\partial x^2}\{r-H_{pl}\}^{\frac{1}{n}+2}}{\left(\frac{1}{n}+1\right)\left(\frac{1}{n}+2\right)2^{\frac{1}{n}}}$$

$$+\frac{\frac{1}{n}\left|\frac{\partial p}{\partial x}\right|^{\frac{1}{n}-2}\frac{\partial p}{\partial x}\frac{\partial^2 p}{\partial x^2}\{H-H_{pl}\}^{\frac{1}{n}+3}}{\left(\frac{1}{n}+1\right)\left(\frac{1}{n}+2\right)\left(\frac{1}{n}+3\right)2^{\frac{1}{n}}r} - \frac{\frac{1}{n}\left|\frac{\partial p}{\partial x}\right|^{\frac{1}{n}-2}\frac{\partial p}{\partial x}\frac{\partial^2 p}{\partial x \partial x^2}\{H-H_{pl}\}^{\frac{1}{n}+1}H_{pl}^2}{\left(\frac{1}{n}+1\right)2^{\left(\frac{1}{n}+1\right)}r} - \frac{\left|\frac{\partial p}{\partial x}\right|^{\frac{1}{n}-1}\frac{\partial H}{\partial x}\frac{\partial p}{\partial x}\{H-H_{pl}\}^{\frac{1}{n}}H_{pl}^2}{2^{\left(\frac{1}{n}+1\right)}r}. \tag{3.20}$$

Now applying the boundary condition (3.13) in Eq. (3.20) and simplifying, we get

$$H\frac{\partial H}{\partial t} = \frac{1}{n}\frac{\partial p}{\partial x}\left|\frac{\partial p}{\partial x}\right|^{\frac{1}{n}-2}\frac{\partial^2 p}{\partial x^2}\frac{(H-H_{pl})^{\left(2+\frac{1}{n}\right)}}{\left(1+\frac{1}{n}\right)2^{\frac{1}{n}}}\left\{\frac{(H+H_{pl})}{2} + \frac{1}{2+\frac{1}{n}}\left(\frac{H-H_{pl}}{3+\frac{1}{n}} - H\right)\right\} + \frac{\partial p}{\partial x}\left|\frac{\partial p}{\partial x}\right|^{\frac{1}{n}-1}\frac{\partial H}{\partial x}\frac{(H-H_{pl})^{\left(1+\frac{1}{n}\right)}(H+H_{pl})}{\left(\frac{1}{n}+1\right)2^{\left(\frac{1}{n}+1\right)}}. \tag{3.21}$$

From Eq. (3.21), the pressure gradient is derived as

$$\left|\frac{\partial p}{\partial x}\right|^{\frac{1}{n}-1}\frac{\partial p}{\partial x}=\frac{g(t)+\int_0^x H(s,t,k)\frac{\partial H(s,t,k)}{\partial t}ds}{\frac{(H-H_{pl})^{\left(2+\frac{1}{n}\right)}}{\left(1+\frac{1}{n}\right)2^{\frac{1}{n}}}\left\{\frac{(H+H_{pl})}{2}+\frac{1}{2+\frac{1}{n}}\left(\frac{H-H_{pl}}{3+\frac{1}{n}}-H\right)\right\}}\quad,\tag{3.22}$$

where $g(t)$ is an arbitrary function of t.

$$\frac{\partial p}{\partial x}=\frac{g(t)+\int_0^x H(s,t,k)\frac{\partial H(s,t,k)}{\partial t}ds}{\frac{(H-H_{pl})^{\left(2+\frac{1}{n}\right)}}{\left(1+\frac{1}{n}\right)2^{\frac{1}{n}}}\left\{\frac{(H+H_{pl})}{2}+\frac{1}{2+\frac{1}{n}}\left(\frac{H-H_{pl}}{3+\frac{1}{n}}-H\right)\right\}}\left|\frac{g(t)+\int_0^x H(s,t,k)\frac{\partial H(s,t,k)}{\partial t}ds}{\frac{(H-H_{pl})^{\left(2+\frac{1}{n}\right)}}{\left(1+\frac{1}{n}\right)2^{\frac{1}{n}}}\left\{\frac{(H+H_{pl})}{2}+\frac{1}{2+\frac{1}{n}}\left(\frac{H-H_{pl}}{3+\frac{1}{n}}-H\right)\right\}}\right|^{n-1},\tag{3.23}$$

The pressure at an arbitrary point along the length of the oesophagus is determined by integrating Eq. (3.23) from the inlet to the arbitrary axial point, it gives

$$p(x,t)-p(0,t)=$$

$$\int_0^x\left[\frac{g(t)+\int_0^w H(s,t,k)\frac{\partial H(s,t,k)}{\partial t}ds}{\frac{(H-H_{pl})^{\left(2+\frac{1}{n}\right)}}{\left(1+\frac{1}{n}\right)2^{\frac{1}{n}}}\left\{\frac{(H+H_{pl})}{2}+\frac{1}{2+\frac{1}{n}}\left(\frac{H-H_{pl}}{3+\frac{1}{n}}-H\right)\right\}}\left|\frac{g(t)+\int_0^w H(s,t,k)\frac{\partial H(s,t,k)}{\partial t}ds}{\frac{(H-H_{pl})^{\left(2+\frac{1}{n}\right)}}{\left(1+\frac{1}{n}\right)2^{\frac{1}{n}}}\left\{\frac{(H+H_{pl})}{2}+\frac{1}{2+\frac{1}{n}}\left(\frac{H-H_{pl}}{3+\frac{1}{n}}-H\right)\right\}}\right|^{n-1}\right]dw,\tag{3.24}$$

so that the pressure difference between two ends of the oesophagus is

$$p(l,t)-p(0,t)=$$

$$\int_0^l\left[\frac{g(t)+\int_0^w H(s,t,k)\frac{\partial H(s,t,k)}{\partial t}ds}{\frac{(H-H_{pl})^{\left(2+\frac{1}{n}\right)}}{\left(1+\frac{1}{n}\right)2^{\frac{1}{n}}}\left\{\frac{(H+H_{pl})}{2}+\frac{1}{2+\frac{1}{n}}\left(\frac{H-H_{pl}}{3+\frac{1}{n}}-H\right)\right\}}\left|\frac{g(t)+\int_0^w H(s,t,k)\frac{\partial H(s,t,k)}{\partial t}ds}{\frac{(H-H_{pl})^{\left(2+\frac{1}{n}\right)}}{\left(1+\frac{1}{n}\right)2^{\frac{1}{n}}}\left\{\frac{(H+H_{pl})}{2}+\frac{1}{2+\frac{1}{n}}\left(\frac{H-H_{pl}}{3+\frac{1}{n}}-H\right)\right\}}\right|^{n-1}\right]dw.\tag{3.25}$$

Now from Eq. (3.22), $g(t)$ is obtained as

$$g(t)=\frac{\int_0^l\left|\frac{\partial p}{\partial x}\right|^{\frac{1}{n}-1}\frac{\partial p}{\partial x}dx-\int_0^l\left\{\int_0^x H(s,t,k)\frac{\partial H(s,t,k)}{\partial t}ds\right\}\left[\frac{(H-H_{pl})^{\left(2+\frac{1}{n}\right)}}{\left(1+\frac{1}{n}\right)2^{\frac{1}{n}}}\left\{\frac{(H+H_{pl})}{2}+\frac{1}{2+\frac{1}{n}}\left(\frac{H-H_{pl}}{3+\frac{1}{n}}-H\right)\right\}\right]^{-1}dx}{\int_0^l\left[\frac{(H-H_{pl})^{\left(2+\frac{1}{n}\right)}}{\left(1+\frac{1}{n}\right)2^{\frac{1}{n}}}\left\{\frac{(H+H_{pl})}{2}+\frac{1}{2+\frac{1}{n}}\left(\frac{H-H_{pl}}{3+\frac{1}{n}}-H\right)\right\}\right]^{-1}dx}.\tag{3.26}$$

For $H_{pl}=0$ and $n=1$, Eqs. (3.23)–(3.26) reduce to corresponding equations for Newtonian fluids derived by Li and Brasseur (1993). This is to be noted that the expression for $H(x,t,k)$, given in Eq. (3.7), is more general than that used by Li and Brasseur (1993).

3.3.1 Time averaged volume flow rate

The volume flow rate for single wave transport in the non-plug region is defined as

$Q(x,t) = 2\beta \int_{H_{pl}}^{H} urdr$, where $\beta = \frac{l}{\lambda}$.

Using Eq. (3.18) and then evaluating the integral, we have

$$Q(x,t) = -2\beta \frac{\partial p}{\partial x}\left|\frac{\partial p}{\partial x}\right|^{\frac{1}{n}-1} \frac{(H-H_{pl})^{\left(2+\frac{1}{n}\right)}}{\left(1+\frac{1}{n}\right)2^{\frac{1}{n}}}\left\{\frac{(H+H_{pl})}{2} + \frac{1}{2+\frac{1}{n}}\left(\frac{H-H_{pl}}{3+\frac{1}{n}} - H\right)\right\}. \tag{3.27}$$

Now we define the following transformations between the wave and the laboratory frames in the non-dimensional form

$$\left.\begin{aligned} &X = x - t, \quad R = r, \quad U(R,X) = u(r,x,t) - 1, \\ &V(R,X) = v(r,x,t), \; q(X) = Q(x,t) - H^2 + H_{pl}^2, \end{aligned}\right\} \tag{3.28}$$

where the parameters on the left side are in the wave frame and those on the right side are in the laboratory frame. The volume flow rate averaged over a period in the laboratory frame for a single wave propagation, is

$\bar{Q}(x) = \frac{1}{\beta}\int_0^{\beta} Q dt$,

which, in view of Eq. (3.28), yields

$$Q = \bar{Q} + H^2 - \frac{1}{\beta}\int_0^{\beta} H^2 dt \ , \tag{3.29}$$

so that, on using Eq. (3.27), the pressure gradient along the axis may be given by

$$\frac{\partial p}{\partial x} = \frac{1}{2^n \beta^n} \frac{-\bar{Q} - H^2 + \frac{1}{\beta}\int_0^{\beta} H^2 dt}{\frac{(H-H_{pl})^{\left(2+\frac{1}{n}\right)}}{\left(1+\frac{1}{n}\right)2^{\frac{1}{n}}}\left\{\frac{(H+H_{pl})}{2} + \frac{1}{2+\frac{1}{n}}\left(\frac{H-H_{pl}}{3+\frac{1}{n}} - H\right)\right\}}\left|\frac{-\bar{Q} - H^2 + \frac{1}{\beta}\int_0^{\beta} H^2 dt}{\frac{(H-H_{pl})^{\left(2+\frac{1}{n}\right)}}{\left(1+\frac{1}{n}\right)2^{\frac{1}{n}}}\left\{\frac{(H+H_{pl})}{2} + \frac{1}{2+\frac{1}{n}}\left(\frac{H-H_{pl}}{3+\frac{1}{n}} - H\right)\right\}}\right|^{n-1} . \tag{3.30}$$

Therefore, the pressure at an arbitrary point along the length of the oesophagus in terms of the time averaged volume flow rate is determined by integrating Eq. (3.30) from the inlet to the arbitrary axial point, and is given by

$$p(x,t) - p(0,t) = \frac{1}{2^n \beta^n} \times$$

$$\int_0^x \frac{-\bar{Q} - H^2(w,t,k) + \frac{1}{\beta}\int_0^{\beta} H^2(w,t,k) dt}{\frac{(H(w,t,k)-H_{pl})^{\left(2+\frac{1}{n}\right)}}{\left(1+\frac{1}{n}\right)2^{\frac{1}{n}}}\left\{\frac{(H(w,t,k)+H_{pl})}{2} + \frac{1}{2+\frac{1}{n}}\left(\frac{H(w,t,k)-H_{pl}}{3+\frac{1}{n}} - H\right)\right\}}\left|\frac{-\bar{Q} - H^2(w,t,k) + \frac{1}{\beta}\int_0^{\beta} H^2(w,t,k) dt}{\frac{(H(w,t,k)-H_{pl})^{\left(2+\frac{1}{n}\right)}}{\left(1+\frac{1}{n}\right)2^{\frac{1}{n}}}\left\{\frac{(H(w,t,k)+H_{pl})}{2} + \frac{1}{2+\frac{1}{n}}\left(\frac{H(w,t,k)-H_{pl}}{3+\frac{1}{n}} - H\right)\right\}}\right|^{n-1} dw. \tag{3.31}$$

For $H_{pl} = 0$, Eq. (3.31) reduces to the corresponding equation for power-law fluids derived by Misra and Pandey (2001).

3.3.2 Local wall shear stress

The local wall shear stress, defined at the wall, is

$$\tau_w(x,t) = \frac{\partial u}{\partial r}\Big|_{r=H} ,$$

which, in view of Eq. (3.18), gives

$$\tau_w = \frac{\frac{\partial p}{\partial x}\left|\frac{\partial p}{\partial x}\right|^{\frac{1}{n}-1}}{2^{\frac{1}{n}}}\left(H - H_{pl}\right)^{\frac{1}{n}} .$$

Using Eq. (3.22), it reduces to

$$\tau_w = \frac{\left(1+\frac{1}{n}\right)\left[g(t)+\int_0^x H(s,t)\frac{\partial H(s,t)}{\partial t}ds\right]}{\left(H-H_{pl}\right)^2\left\{\frac{\left(H+H_{pl}\right)}{2}+\frac{1}{2+\frac{1}{n}}\left(\frac{H-H_{pl}}{3+\frac{1}{n}}-H\right)\right\}}, \tag{3.32}$$

where H is defined by Eq. (3.7) and $g(t)$ by Eq. (3.26).

3.4 Results and discussions

In order to investigate the effects of various parameters such as flow behavior index, amplitude dilation and the plug flow width on swallowing of Herschel-Bulkley fluid, we plot graphs for local pressure along the axis. The case considered here is free pumping which is obtained merely by setting zero pressure at the two ends of the oesophagus. When a non-Newtonian fluid swallows, only one bolus moves practically at a time in the oesophagus. Therefore, for the pictorial demonstration, we consider single bolus swallowing in the oesophagus although it can accommodate as many as three boluses at a time as per our consideration.

The primary concern is the pressure distribution along the axis when a bolus travels down the oesophagus towards the cardiac sphincter. Since the mathematical model involves expressions that cannot be integrated by classical methods, the only way out is to go for numerical solution. Moreover, the values of all the dimensionless parameters are merely suitable assumptions to facilitate qualitative investigation.

3.4.1 Effect of yield stress on flow dynamics

When the fluid enters the oesophagus through its inlet, a bolus is created which moves with the wave. A bolus is considered to be confined within one peristaltic wavelength; and so it

appears at different positions at different instants. Since this is a qualitative investigation, no physiological data have been collected to validate the assumptions.

The first prominent aspect required to be investigated is the effect of yield stress on the flow dynamics of peristaltic transport when the wave amplitude increases exponentially. We set $\emptyset = 0.7,\ k = 0.01,\ n = 1.1$ and H_{pl} is varied in the range 0.0-0.08. The results are depicted in Fig. 3.3.

At $t = 0.0$ (Fig. 3.3(a)) it is observed that greater the yield stress, higher is the fall in pressure revealing a larger requirement of pressure. For the instants $t = 0.25 - 2.0$ (Figs. 3.3(b)-(f)), pressure gradient behind the bolus is positive which shows that the bolus does not move in the backward direction. It is observed that in all such cases, pressure required for swallowing is more for the higher yield stress. When the bolus progresses, it is observed that the requirement of pressure, adequate to carry the bolus forward, increases. This is revealed in Figs. 3.3(b)-(f). This is to be noted that when $t = 0.5$, the pressure requirement is least but the pressure requirement is the maximum in the lower oesophagus. This is in confirmation with the finding of Kahrilas et al. (1995), who located the highest pressure in the lower oesophagus. We can thus conclude here that thicker the plug flow region, larger is the pressure required for flow, which further increases as the wave amplitude dilates with moving bolus.

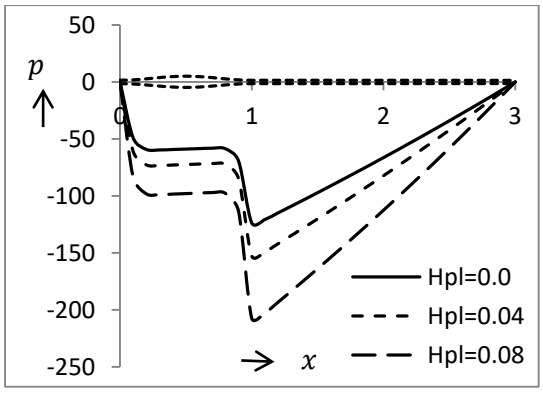

(a) *t = 0.0*

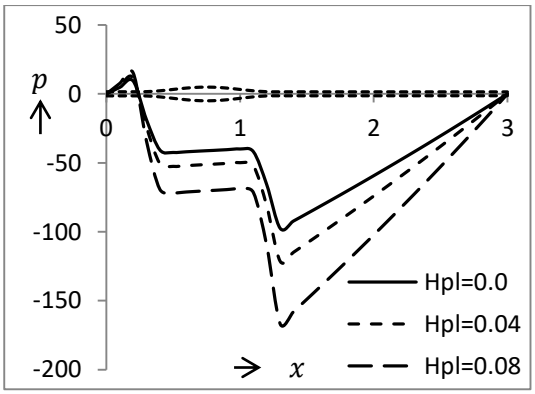

(b) *t = 0.25*

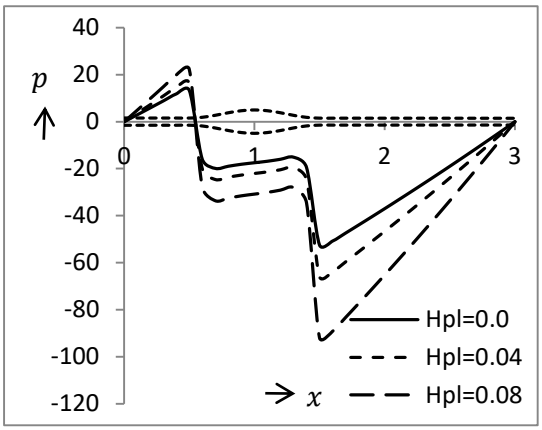

(c) *t = 0.50*

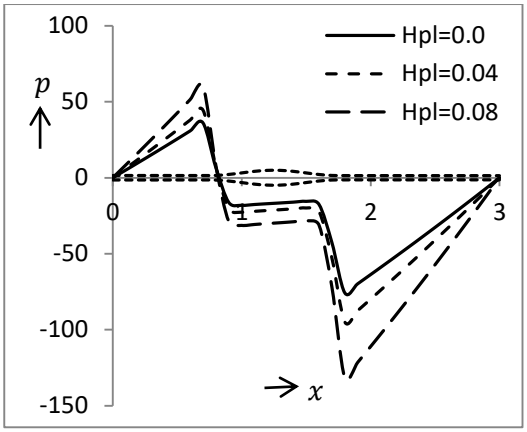

(d) *t = 0.75*

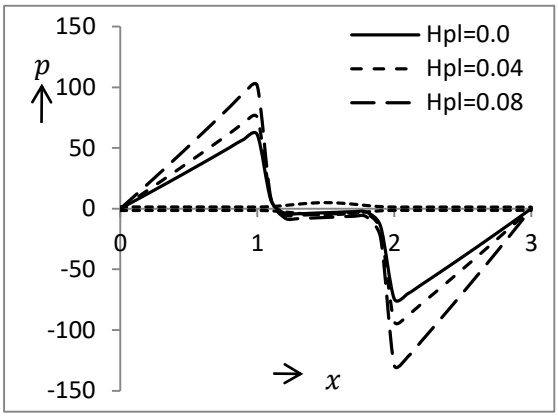

(e) *t = 1.0*

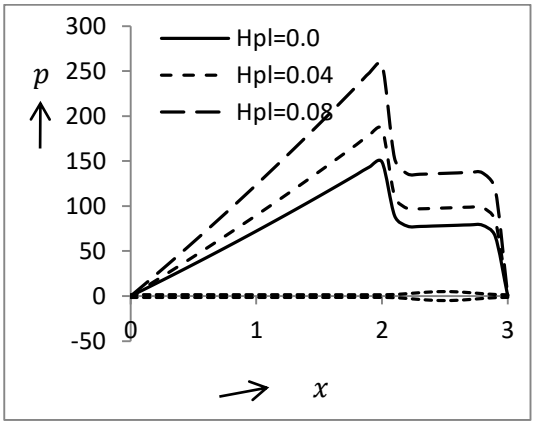

(f) *t = 2.0*

Fig. 3.3(a-f) *Pressure distribution along axial distance at different instants* ($t = 0.0, 0.25, 0.50, 0.75, 1.0, 2.0$) *showing the effect of radius of the plug flow region* H_{pl}. *Other parameters are taken as* $\emptyset = 0.7, n = 1.1, k = 0.01$.

3.4.2 Effect of flow behaviour index

Herschel-Bulkley fluid is a very general type of fluid which carries at a time properties of several types of fluids. For investigation, we assume three values $n = 0.9, 1, 1.1$. The values of n, which can have much larger variations, are randomly picked up. Though very close, the three values represent three different types of fluids, viz., pseudo plastic, Newtonian and dilatants respectively if the yield stress is considered to be zero. These names are used only when there is no yield stress which causes a plug flow region in the middle of the flow. However, we can call them pseudo plastic and dilatant. For $n = 1$ with yield stress, the fluid is known as Bingham fluid. The dilation parameter is fixed as $k = 0.01$ and the plug flow region is set as $H_{pl} = 0.01$ for investigating the impact of flow behavior index n.

The pressure curves corresponding to $t = 0.0$ given in Fig. 3.4(a) reveal that the pressure falls sharp at its tail to facilitate the bolus to travel down the oesophagus. This is possible only when the local pressure gradient is negative. But beyond the head of the wave, pressure increases to prevent any retrograde flow. It is observed that the depression of pressure increases with the increasing flow behaviour index, indicating thereby that the pressure required to drag the fluid is more for $n > 1$ and less for $n < 1$ (less than that for Bingham fluid ($n = 1$)). But at $t = 0.25$ (Fig. 3.4(b)), pressure increases as we move along the length of the oesophagus from the upper sphincter. As soon as it reaches the tail of the wave, it starts falling, reaches the minimum at the head of the wave, and then rises linearly to maintain a pressure balance at the two ends. At $t = 0.50$, pressure rises again at the tail of the bolus as it travels some more distance along the oesophagus which is shown in Fig. 3.4(c). Now pressure dips in the similar manner to maintain its motion towards the lower oesophageal sphincter, and then rises to zero at the lower oesophageal sphincter. Pressure distribution along the axis of the bolus and within it, is almost the same as the previous case. A similar trend is observed at $t = 0.75$ (Fig. 3.4(d)) as well as at $t = 1.0$ (Fig. 3.4(e)) except that the magnitude of the two peaks which differ according to the position of the wave. At $t = 1.0$, completes one cycle. Plot for $t = 2.0$ given in Fig. 3.4(f) reveals that the lower oesophageal sphincter is about to deliver the food bolus to stomach where the pressure distribution is completely reversed as compared to that at the upper oesophageal sphincter. Throughout the journey of bolus, pressure distribution remains similar for dilatant, Newtonian and pseudo plastic motion of the fluid apart from the fact that a plug flow region has been maintained. Quantitatively, differences of the pressures corresponding to the three cases are quite large. Dilatant fluid requires larger pressure than partly Newtonian nature (which is Bingham fluid here) while the pseudo plastic nature requires lesser pressure.

Achalasia causes inadequate lower oesophageal sphincter relaxation. As a consequence of inadequate lower oesophageal sphincter relaxation oesophageal clearance is delayed. Therefore, a possible treatment for patients with inadequate lower oesophageal sphincter relaxation may be that this is overcome through drugs or operation (Spechler and Castell, 2001). Our investigation reveals that swallowing of pseudo plastic fluid requires lesser pressure in compression to that of Bingham fluid or dilatant fluid. Hence, an outcome of the present analysis favours feeding of pseudo plastic fluids for patients suffering from achalasia.

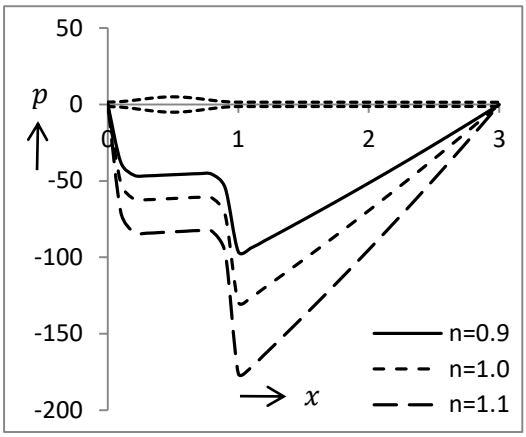

(a) *t = 0.0*

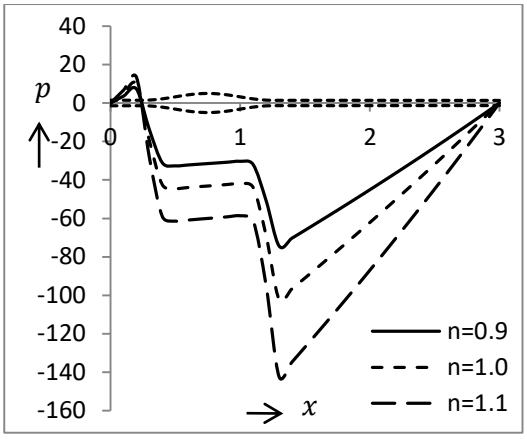

(b) *t = 0.25*

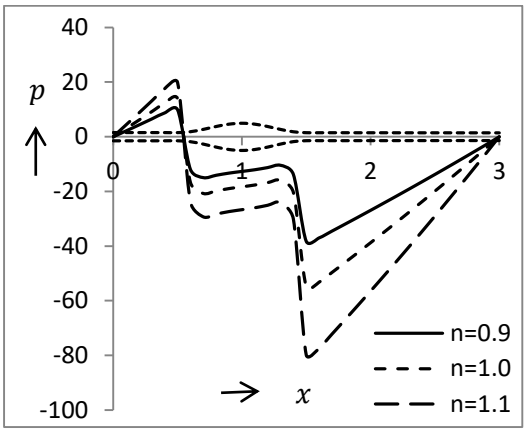

(c) *t = 0.50*

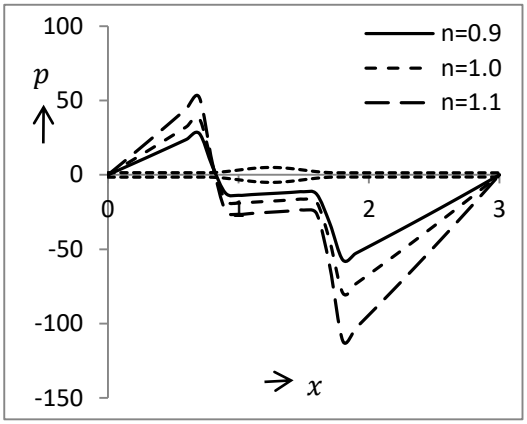

(d) *t = 0.75*

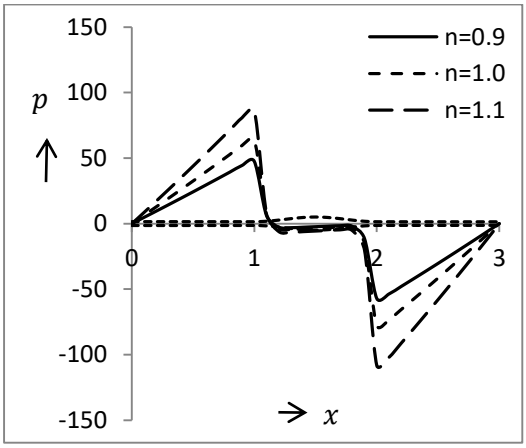

(e) *t = 1.0*

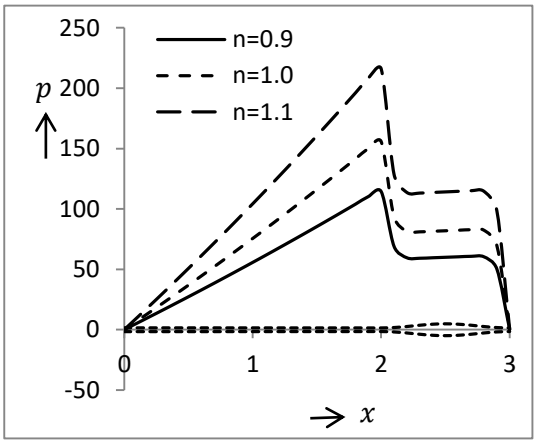

(f) *t = 2.0*

Fig. 3.4(a-f) *Pressure distribution along axial distance at different instants* ($t = 0.0, 0.25, 0.50, 0.75, 1.0, 2.0$) *showing the effect of flow behavior index n. Other parameters are taken as* $\emptyset = 0.7$, $k = 0.01$, $H_{pl} = 0.01$.

3.4.3 Effect of dilating wave amplitude

The effect of dilating wave amplitude on the flow dynamics is depicted in Fig. 3.5. The comparison of plot at $t = 1.0$ to $t = 2.0$ (Fig. 3.5) show that unlike the case of peristaltic wave with constant amplitude (Figs. 3.5(a)-(f)), corresponding to $k = 0.0$), the difference between the maximum and the minimum pressures becomes larger when wave-amplitude dilates (Figs. 3.5(a)-(f), corresponding to $k = 0.02$ and $k = 0.03$), i.e., pressure distribution for dilating amplitude is observed to differ from that for constant amplitude. An observation of Figs. 3.5(a) and 3.5(f) reveals that pressure gradients, corresponding to $k = 0.02$ and $k = 0.03$, are greater in magnitude in the lower oesophageal part than that in the upper oesophageal part and also, the pressure rises most in the lower part of the oesophagus. It conforms the experimental observations (Kahrilas et al., 1995) of high pressure zone in the lower oesophageal part.

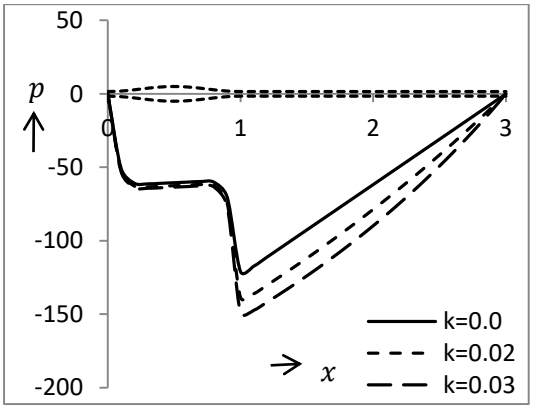

(a) *t = 0.0*

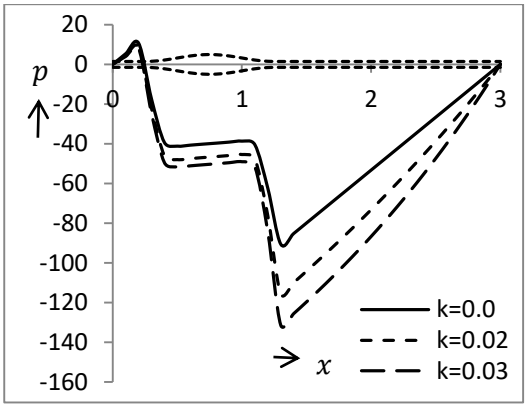

(b) *t = 0.25*

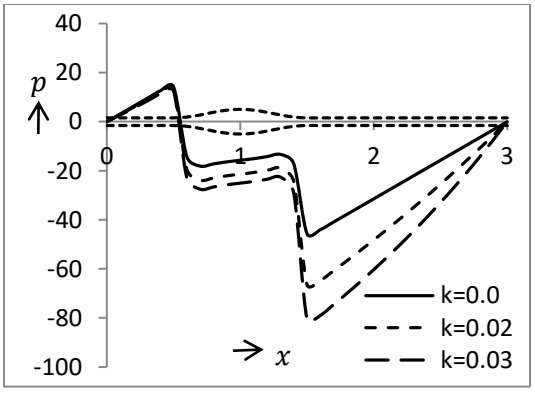

(c) *t = 0.50*

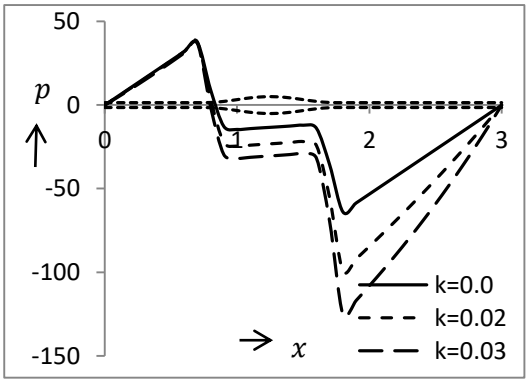

(d) *t = 0.75*

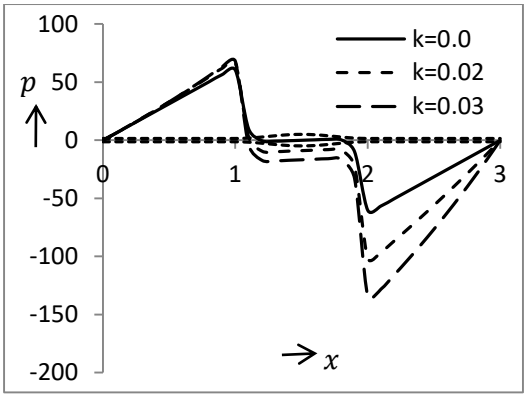

(e) *t = 1.0*

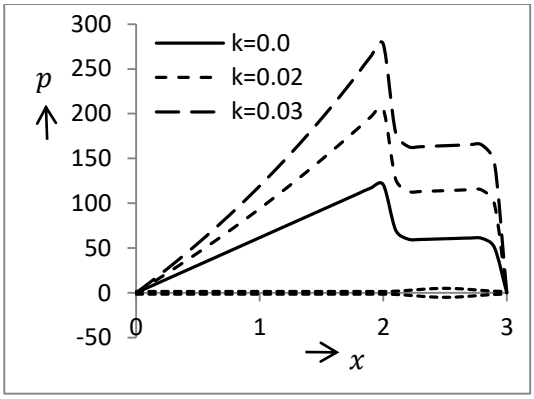

(f) *t = 2.0*

Fig. 3.5(a-f) *Pressure distribution along axial distance at different instants* ($t = 0.0, 0.25, 0.50, 0.75, 1.0, 2.0$) *showing the effect of dilation parameter* k. *Other parameters are taken as* $\emptyset = 0.7,\ H_{pl} = 0.01,\ n = 1.1$.

3.5 Conclusion and physical interpretation

The aim of this investigation is to learn the effect of dilating wave amplitude on the non-Newtonian nature of the fluid flowing in the oesophagus. The non-Newtonian nature is here characterized by the presence of a plug flow region arising out of yield stress and variation of flow behavior index making it pseudo plastic or dilatant depending on whether the flow behavior index is less than or greater than one. All these characteristics give it the name Herschel-Bulkley fluid. The presence of a plug flow region requires more pressure to be exerted by the oesophageal wall on the fluid swallowing inside it. Dragging by the dilating wave amplitude increases it further. This conforms the experimental observations (Kahrilas et al., 1995) of high pressure zone in the lower oesophageal part.

When the fluid is pseudo plastic (i.e. $n < 1$) pressure required for swallowing is less than that for Newtonian fluids. Dilatant fluid (i.e. $n > 1$) requires much more pressure than pseudo plastic and Newtonian as well, for swallowing. All the characteristics put together makes the assessment very much complicated.

It is also observed that the magnitude of pressure along the oesophagus increases with increasing flow behaviour index which reveals that swallowing of pseudo plastic fluid is easier than that of dilatant fluid. It is also observed that for exponentially increasing wave-amplitude, pressure keeps increasing along the entire length of the oesophagus; and finally towards the end of the oesophageal flow, it is at the peak. It is observed that the pressure distribution is dependent on the position of the wave in the oesophagus. The spatial rate of change in the pressure difference is found to be much greater when the wave originates at the inlet and terminates at the outlet of the oesophagus than when the wave

travels in the middle (Figs. 3.3-3.5). This may be attributed to the fact that the pumping action does not take place along the entire length of the oesophagus uniformly. The rate of change is more in the vicinity of the inlet and the outlet. It is further concluded that the pressure difference at a given axial position is more for a dilatant fluid than that for a pseudo plastic fluid. The pressure-difference corresponding to a Bingham fluid falls in between these two values.

This is also concluded on the basis of the present analysis that feeding of pseudo plastic fluids are preferable to the patients suffering from achalasia.